

A Spatial Deconstruction Behavioural Model for Pedestrian Dynamics

Yao Xiao

^aSchool of Intelligent System Engineering, Sun Yat-Sen University, Shenzhen, China

Abstract

How to reproduce realistic motion in simulations has always been a fundamental problem for pedestrian dynamics, and a critical challenge for current studies is the natural correlation of the movement choices and the human behaviours. To advance the study, we deconstruct the two-dimensional space of pedestrian crowds with a behavioural motion network on basis of Voronoi diagram and Delaunay diagram, and accordingly formulate a behavioural model considering both the long-term route choice and the real-time velocity choice. The comparisons between simulation results and real-world movements suggest that the behavioural model can not only deal with traditional scenarios but also be capable of describing well-agreed movements in challenging conflicting situations. The spatial deconstruction idea provides a geometric perspective to recognize and reproduce the pedestrian behaviours, and it can further benefit the understanding and realization of pedestrian dynamics and even robot navigation.

Keywords: Pedestrian Dynamics, Behavioural Model, Motion Network, Circle Antipode Experiment

1. Introduction

Considering the growing frequency of public activities and the increasing congestion extent at daily peak commuting times, the investigation of pedestrian crowds has attracted the attention of many researchers. These studies have benefited the design of public facilities (Helbing et al., 2005) as well as the organization of crowd activities (Bain & Bartolo, 2019). Among these researches, a fundamental topic is about how to reproduce realistic pedestrian motion behaviours, especially in complex situations.

Different types of microscopic modeling ideas (Helbing & Molnar, 1995; Blue & Adler, 2001; Moussaid et al., 2011; Van Den Berg et al., 2011; Alexandre et al., 2016; Xiao et al., 2016) have been proposed to simulate pedestrian crowds in a two-dimensional space. The widely-used social force model (Helbing & Molnar, 1995; Helbing et al., 2000) regards pedestrians as Newton's Second Law based particles driven with a combination of a driving force (the desire to reach a target), social forces (the untouched psychological interaction) and contact forces (the touched physical interaction). Through reviewing the traditional model, a heuristic model (Moussaid et al., 2011) further introduces two simple cognitive procedures based on the distance of obstructions to adapt the pedestrian directions and speeds. Meanwhile, other modeling ideas such as the cellular automata model (Blue & Adler, 2001; Fu et al., 2018), velocity obstacle model (Van Den Berg et al., 2011; Douthwaite et al., 2019), machine learning method (Alexandre et al., 2016; Ma et al., 2019), Voronoi model (Xiao et al., 2016) are proposed and attempted. In spite of the reproduction of well-agreed fundamental diagrams and many self-organized phenomena, human behaviours are still not properly

*E-mail address: xiaoyao9@mail.sysu.edu.cn

considered in current models. First, a real pedestrian considers not only the perceptible real-time velocity choice but also the latent long-term route choice among dynamic pedestrians. The lack of route choice consideration would lead to an imperfect motion mechanism and create an insuperable gap between simulation and reality (e.g., the lack of roundabout strategies in complex situations). Second, current models rely too much on particle properties (e.g, individual repulsion) rather than directly introducing realistic pedestrian motion strategies (e.g., following other pedestrians or making a detour). For these problems, how to deconstruct the flexible pedestrian space and find the corresponding behaviour-based route choice is the critical issue.

Herein, a motion network based on the Voronoi diagram and its dual graph Delaunay diagram (Fortune, 1987) is proposed. Through a combination between the geometric features of the motion network and the behavioural characteristics of pedestrian dynamics, a series of systemic and behavioural routes are recognized and defined. Accordingly, a behavioural model considering both the long-term route choice and the real-time velocity choice is proposed.

The rest of paper is organized as follows. Section 2 introduces the behavioural motion network and describes the formulation of the behavioural model. In Section 3, simulations of both traditional and challenging scenarios are conducted. Section 4 discusses the model results and the potential improvements in the future.

2. Model

The modeling of pedestrian dynamics is usually simplified into a two-dimensional space, and the core problem (see Eq. 1) for pedestrian P_i is about how to reach the destination D_i while considering geometries G and pedestrians (P_1, P_2, \dots, P_n) .

$$\mathbf{s}_i = (\mathbf{r}_i, \mathbf{v}_i) = f(P_1, P_2, \dots, P_n; \mathbf{G}; D_i) \quad (1)$$

Inspired by the practical pedestrian decision process, the motion strategy \mathbf{s}_i of pedestrian P_i is divided into two phases, the long-term route choice \mathbf{r}_i which predicts the anticipatory motion strategic route in the foreseeable future, and the real-time velocity choice \mathbf{v}_i which indicates the present velocity direction and speed (Fig.1-a). Namely, the route choice guides the instantaneous velocity choice, while the velocity choice reflects the anticipatory route choice. In a former work (Xiao et al., 2016), the decision process of the real-time velocity choices is initially formulated. Here, the original real-time model is extended, and the long-term route choice and the real-time velocity choice are integrated together.

2.1. Long-term route choice

The spatial deconstruction can contribute to the recognition of the pedestrian status and the topological relationship among pedestrians, and the long-term route choice behaviours can also be significantly benefited. For this reason, a pedestrian motion network (see Fig.1-b) is formulated at each time step based on the Voronoi diagram of the pedestrians and its dual graph Delaunay diagram.

Motion network. The motion network contains four types of nodes and five types of segments, and it can be divided into three sub-networks (see Fig.1-c). The Delaunay network describes a kind of topological relationship

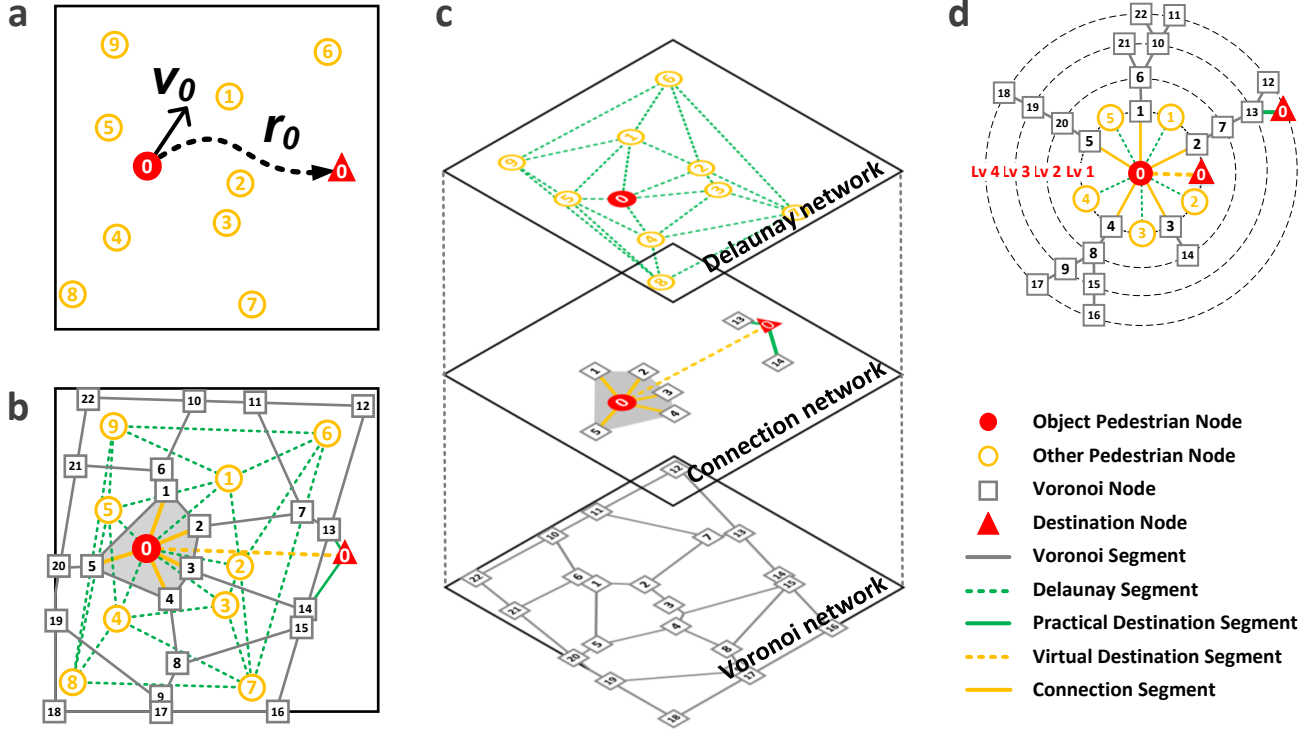


Figure 1: **Pedestrian dynamics problem and motion network.** **a**, Sketch map of pedestrian motion problem. 10 pedestrians represented by circles are initialized in a closed square space. The object pedestrian P_0 needs to leave for the corresponding destination D_0 , and his/her supposed velocity choice v_0 and route choice r_0 are shown by solid and dashed arrows, respectively. **b**, Pedestrian motion network. **c**, Sub-networks of pedestrian motion network. **d**, Feasible routes of object pedestrian. Note that these feasible routes are obtained by finding the minimum time cost and considering the route segment counts.

(Ballerini et al., 2008) between one pedestrian and his/her adjacent pedestrians (e.g., the neighbors of pedestrian P_0 include pedestrians P_1, P_2, P_3, P_4 , and P_5), and the potential pedestrian following direction pattern can be accordingly inspired. The Voronoi network indicates the intermediate passageway between two pedestrians (e.g., Voronoi segment N_2N_7 represents the intermediate passageway of pedestrian P_1 and P_2), and the potential pedestrian crossing, overtaking and detour pattern can be obtained. The connection network links the pedestrian, the destination and the Voronoi nodes, as well as the Voronoi network and the Delaunay network. On basis of the integrated motion network, a series of routes can be found from a pedestrian to his/her destination.

Perception scope. Generally, it is impractical for a pedestrian to schedule a tortuous route in a large crowd, and an overly long planned route might not make sense in the time-varying dynamic surroundings. As a result, the real perception scope of a pedestrian is usually limited, and it can be implemented by introducing a threshold value of route length. Three types of route choices among the potential routes are found and defined according to the first segment of route, i.e., destination pattern (virtual destination segment), following pattern (Delaunay segment) and detour pattern (connection segment). Since only the detour pattern is considered to be an aggressive behaviour in the model, all the segment lengths of the routes except for the detour routes are limited to be only one.

In practical, a pedestrian generally precisely calculates the cost in the perception scope and roughly estimates the potential cost to the goal outside the perception scope. Therefore, the A* search algorithm (Hart et al., 1968)

is introduced and modified as Eq. 2 to find the optimal strategic route \mathbf{r}_i^* of pedestrian P_i from the feasible route set \mathbf{R}_i as shown in Fig. 1-d.

$$\mathbf{r}_i^* = \arg \min_{\mathbf{r}_i \in \mathbf{R}_i} \left(\frac{\delta^r}{v_i^*} \cdot \left(\sum_{k=1}^K \delta^s L_i^k + \sigma_i D_{\mathbf{r}_i} \right) \right) \quad (2)$$

where L_i^k and $D_{\mathbf{r}_i}$ respectively represent the length of k th route segment inside the perception scope and the Euler distance from the tail node of the strategic route to the destination outside the perception scope. v_i^* indicates the speed determined according to the first segment of route, and σ_i is a detour coefficient (see Appendix A). $\delta^s = \exp(\sum_{m=1}^{M^s} \phi_m \lambda_m^s)$ is a penalty term for the segment, and ϕ_m is the type judgment term (i.e., if the segment meets the required type, $\phi_m = 1$, otherwise, $\phi_m = 0$). $\delta^r = \exp(\sum_{m=1}^{M^r} \lambda_m^r)$ is a penalty term for the strategic route.

In our model, two types of segment penalties and one type of route penalty are taken into consideration. For the Delaunay segment which indicates the following behaviour, the synergy effect with the following target is formulated as, $\lambda_1^s = \alpha_1 \cdot ((1 - \mathbf{e}_i \cdot \mathbf{e}_i^f) + (1 - \mathbf{e}_i^0 \cdot \mathbf{e}_i^f))$, where \mathbf{e}_i^0 , \mathbf{e}_i and \mathbf{e}_i^f respectively indicate the unit vector of the pedestrian desired direction, the pedestrian velocity direction and the following target's velocity direction. The Voronoi segment indicates the passageway between two adjacent pedestrians from a geometrical view. To reflect the difficulty level of the across behaviour, the time penalty is formulated as, $\lambda_2^s = \alpha_2 \cdot d_i^r / w^2$, where d_i^r and w are respectively the radius of pedestrian circle and the width between the adjacent pedestrians. The type of route penalty is proposed to realize the conflict avoidance behaviour, $\lambda_1^r = \beta_1 \cdot n(A)$, $A = \{\mathbf{x}_{ob} | \|\mathbf{x}_{ob} - \mathbf{x}_c\| < 2d_i^r, \mathbf{x}_{ob} \in \mathbf{X}_{ob}\}$, \mathbf{x}_c is the location of tail node of current route, and \mathbf{X}_{ob} contains the existing tail nodes of other strategic routes. The other parameters here are respectively set as, $\alpha_1 = 1$, $\alpha_2 = 3$ and $\beta_1 = 5$. Note that further terms can also be added in the route and segment penalty formula to describe the related impacts.

2.2. Real-time velocity choice

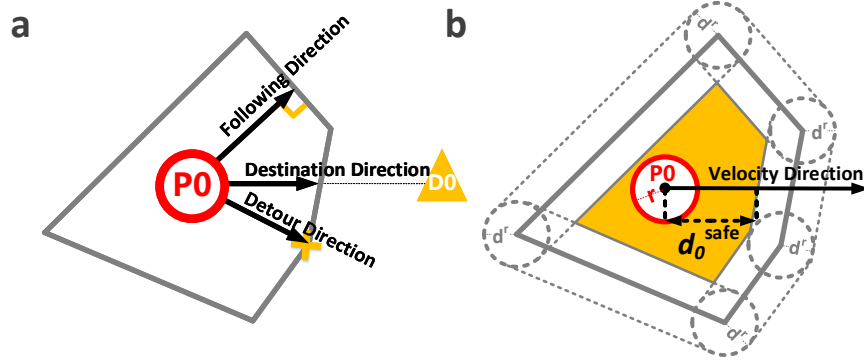


Figure 2: **Sketch map of Voronoi cell and velocity choice.** a, Direction choices. In the Voronoi cell of pedestrian P_0 , the three types of direction choices including, destination direction, following direction and detour direction are marked. b, Safe distance and speed determination.

The process of the real-time velocity choice for pedestrian P_i can be divided into two parts (Moussaid et al., 2011), the determination of direction \mathbf{e}_i^* and the determination of speed v_i^* .

Direction choice. The three types of the first segments in route choice just correspond to three direction choice behaviours, respectively. In a Voronoi cell (see Fig. 2-a), the Delaunay segment perpendicular to the

corresponding Voronoi cell boundary denotes the direction to adjacent pedestrians which is a general following direction \mathbf{e}_{follow} . The connection segment pointing to the Voronoi node represents the direction between two adjacent pedestrians which is theoretically an across or detour direction choice \mathbf{e}_{detour} . The virtual destination segment directly corresponds to the direction choice to the destination \mathbf{e}_{dest} . In summary, the three alternative direction choices for the optimal direction are introduced as $\mathbf{e}_i^* \in \{\mathbf{e}_{dest}, \mathbf{e}_{follow}, \mathbf{e}_{detour}\}$, and our experimental investigations (Xiao et al., 2018) show that the combination of the three direction choices is able to describe most motion behaviours in pedestrian crowds. The pedestrian velocity direction is determined according to the long-term route choice, and the direction unit vector is $\mathbf{e}_i^* = \mathbf{e}(\mathbf{r}_i^*)$.

Speed choice. Since the corresponding Voronoi cell of each pedestrian (e.g., the gray Voronoi cell area in Fig.1-b) contains all of the points closer to that pedestrian than to any other, it is defined as the personal space. Based on this, the safe distance d^{safe} is defined as the maximum distance to the boundary of the personal space along the velocity direction (see Fig. 2-b where the pedestrian is represented by a circle). Accordingly, the speed of pedestrian P_i is determined as, $v_i^* = \min(v_i^0, 2(d_i^r + d_i^{safe})/\tau_i)$, where v_i^0 is the desired speed. In addition, a velocity obstacle concept (Fiorini & Shiller, 1998; Van Den Berg et al., 2011) can be applied to further improve the practical conflict avoidance performance.

A second-order (acceleration) motion equation (Eq. 3) is introduced (Helbing & Molnar, 1995; Helbing et al., 2000) to describe the velocity change of pedestrian P_i at time step t .

$$\frac{d\mathbf{v}_i(t)}{dt} = \frac{\mathbf{e}_i^* \cdot v_i^* - \mathbf{v}_i(t)}{\tau_i}, \quad (3)$$

In the equation, the relaxation time is set as $\tau_i = \ln(1 + 2d_i^r + 2d_i^{safe})$, hence the pedestrians can be more responsive in critical situations.

3. Results

The spatial deconstruction based behavioural model can reproduce realistic crowd movements in different situations. In the section, we firstly test the model performance with several traditional indexes and then explore the model practicality in the challenging circle antipode experiments.

3.1. Traditional scenarios

The fundamental diagram (Seyfried et al., 2005) mainly describes the relationship between macroscopic parameters (e.g. density, velocity and flow), and it is currently a most widely-used indicator (Boltes et al., 2019) to validate the pedestrian model performance. Fig. 3-a shows the well-agreed velocity-density curve pattern between the simulated results and the experimental results (Older, 1968; Weidmann, 1993).

Another critical model reliability indicator is related to the reproduction of the self-organized phenomena (Mousaid et al., 2011; Helbing et al., 2005; Helbing & Johansson, 2009), among which the lane formation (Seyfried et al., 2005; Helbing et al., 2005) in bi-directional flow is a representative one. The model reproduces obvious crowd lanes in the bi-directional flow scenarios after a simulation of 20 s as shown in Fig.3 - b. Besides, more variety of the self-organized phenomena (e.g., stop-and-go wave, and arching phenomenon) as well as critical situations (e.g., U-shape obstacle, and aggressive pedestrian) can be captured by the behavioural model.

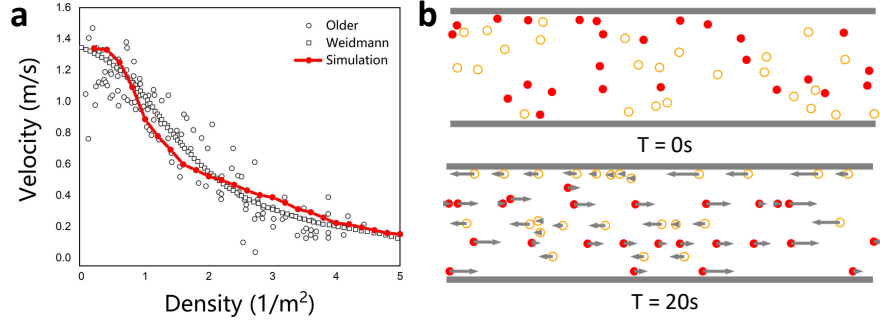


Figure 3: **Simulation performance in traditional scenarios.** Pedestrians are randomly initialized in a 15×5 m corridor with periodic boundaries, and the desired velocity is normally distributed as $v^0 \sim N(1.35, 0.5)$. **a**, Velocity-density relation in the uni-directional flow. The simulation results are obtained by averaging the pedestrian velocities, and each data point responds to a certain participant number. **b**, Lane formation in the bi-directional flow. Half of the participants (orange hollow circles) head toward the left end of the corridor and the rest (red solid circles) head for the other side. The arrows represent the velocity directions.

3.2. Circle antipode Scenarios

The route navigation and conflict avoidance behaviours in crowds are challenging topics in the simulations of pedestrian dynamics. To have an ideal research scenario, the circle antipode experiments in which the pedestrians are uniformly initialized on the circle and required to leave for the antipode position simultaneously are designed. On 22 May 2019, we organized a series of repeated circle antipode experiments at the square before a teaching building in Beijing Jiaotong University. A total of 64 participants are included in the experiments, and they are all students aged between 18 to 28 and height between 170 cm to 180 cm. On top of the teaching building, a high-resolution camera is set to record the whole experiment, and PeTrack (Boltes & Seyfried, 2013; Boltes et al., 2010) is then applied to recognize the pedestrians in the video and obtain the corresponding trajectories on the ground (see Fig.4-a). In the circle antipode experiment, all the 64 participants are initialized on a circle of 10m radius. After a short pause when all participants respectively reached their destination, the participants are simultaneously required to leave for the antipode position again, and the process repeated 20 times except for several warm-up experiments. There are two significant characteristics in the experiments that would benefit the model validation. First, the shortest routes of pedestrians converge on the center position of the circle, so the central region is likely to be a conflicting area. This knowledge can significantly benefit the research of route navigation and conflict avoidance behaviours. Second, except for the pedestrian heterogeneities, the motion conditions for each participant are symmetric in the experiments (e.g., symmetric starting position, symmetric destination position, and symmetric surrounding). Thus, it's a kind of repeat experiment for the participants (i.e., 64 repeated samples are obtained in the experiment with 64 participants), and the indeterminate features of the pedestrian behaviours can be greatly overcome.

In Fig.4-b, the original trajectories as well as the rotated trajectories (rotated to the same starting point) are extracted and processed. It's easy to find that the pedestrian route choices especially the detour choices have been made at the very beginning when there is no actual conflicts in the way to the destination. Namely, the intelligent individuals in our experiments can not only deal with the conflicts at present but also predict the future potential conflicting situation among pedestrian crowds. Considering the fundamental mechanism of traditional models,

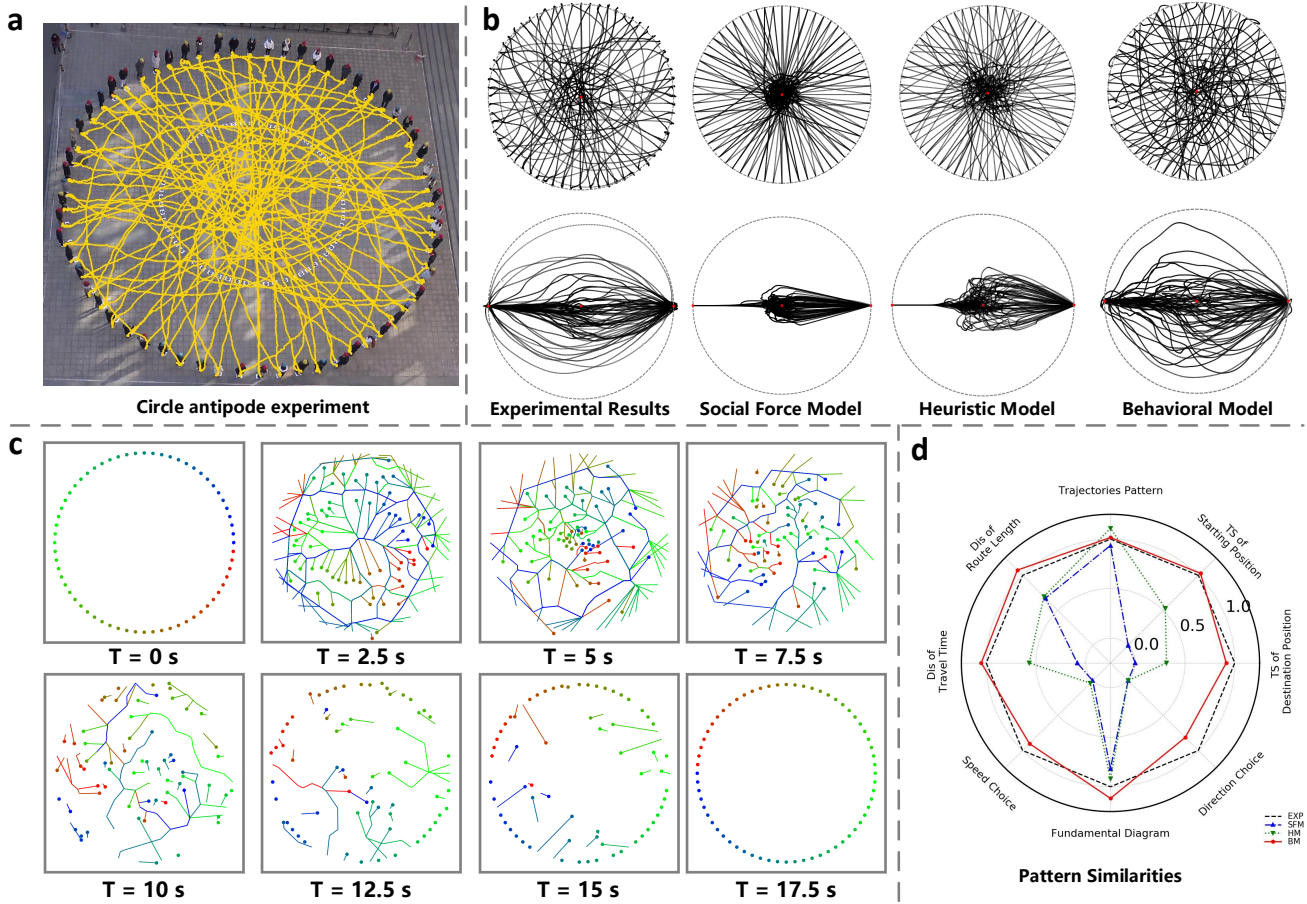


Figure 4: **Circle antipode experiments and simulations.** **a**, Empirical trajectories of a sample circle antipode experiment. The yellow lines represent the ground trajectories during the experiments. **b**, Trajectory comparisons among experiments and different models. Considering the symmetric experimental condition, the original trajectories above are further rotated to the same starting position on the left side and the same destination position on the right side. **c**, Snapshots of the behavioural model simulation. **d**, Pattern similarities between experiments and simulations. A total of 8 indexes are introduced for evaluation and more details can be found in Xiao et al. (2022). The data necessary to support the findings of this manuscript are available in a public repository (<https://github.com/rickyspy/Behaviour-Model-Data>)

it's too challenging to reproduce well-agreed pedestrian behaviours in the circle antipode experiments (see the trajectories of the social force model (Helbing & Molnar, 1995; Helbing et al., 2000) and heuristic model (Moussaid et al., 2011) in Fig.4-b.

On the contrary, the proposed behavioural model can be used for the extremely conflicting situations and reproduce well-agreed trajectory patterns as shown in Fig.4-b. From further snapshots of the behavioural model simulation in Fig.4-c (including pedestrian and his/her corresponding route choice), we can find two major types of route choices. Some just walk through the conflicting central region and the others tend to detour from the relaxed region on the outside. In fact, the heterogeneous types of route choices in the simulation are consistent with the empirical results.

To further quantitatively measure the pattern similarities between simulations and experiments, we introduce a comprehensive evaluation framework containing 8 sets (4 types) of indexes (see Fig. 4-d). The pattern sim-

ilarities of repeated experiments(EXP), social force model(SFM)([Helbing et al., 2000](#); [Helbing & Molnar, 1995](#)), heuristic model(HM)([Moussaïd et al., 2011](#)) and our behavioural model(BM) are investigated within the evaluation framework. Note that there is also a pattern similarity among repeated experiments due to the indeterminacy of pedestrian behaviours, and each index is normalized with the empirical results in repeated experiments. As a result, a greater pattern similarity indicates a better performance, and a score of 1 theoretically indicates a similar performance as the repeated empirical experiments. In Fig. 4-d, a slight advantage of the heuristic model is found for the trajectories pattern index, and the side choice behaviour at the beginning of the circle antipode experiments is believed to be the critical cause ([Xiao et al., 2022](#)). Nevertheless, our behavioural model shows a great advantage to reproduce realistic results in the circle antipode experiments for most indexes.

4. Discussion

The proposed pedestrian behavioural model can not only deal with the existed conflicts and make practical avoidance, but also anticipate the potential conflicting areas in the future and schedule the route in advance. The combination of the long-term route and real-time velocity choices on basis of the motion network formulates the foundation of these complicated pedestrian walking behaviours. In addition to agreeing closely with the traditional simulation results, the behavioural model can reproduce more reliable crowd movements in the challenging circle antipode experiment which requires macroscopic level motion planning.

This work provides a geometric spatial deconstruction approach to understand and combine pedestrian behaviours, and both the route and velocity choice modules on basis of the spatial deconstruction approach can be further developed. For instance, it's not hard to find more modeling possibilities based on the current velocity determination module which contains three discrete direction choices (i.e., destination direction, detour direction, and following direction). Also, the current route choice module in our model is still simplified, and more route planning approaches based on the formulated motion network is likely to be practicable and promising.

The proposed spatial deconstruction behavioural model can contribute to the understanding and development of robot navigation ([Khambhaita & Alami, 2020](#); [Pandey et al., 2017](#)). What's more, the widely-applied deep learning methods show great potential for predicting pedestrian trajectories([Alexandre et al., 2016](#); [Zhang et al., 2019](#)). Incorporating these methods into our behavioural model can benefit the accuracy improvement.

Acknowledgment

We wish to acknowledge the support from the National Natural Science Foundation of China (Grant No. 72101276).

References

References

Alexandre, A., Kratarth, G., Vignesh, R., Alexandre, R., Li, F.-F., & Silvio, S. (2016). Social lstm: Human trajectory prediction in crowded spaces. In *Proceedings of the IEEE Conference on Computer Vision and Pattern Recognition* (pp. 961–971).

- Bain, N., & Bartolo, D. (2019). Dynamic response and hydrodynamics of polarized crowds. *Science*, *363*, 46–49.
- Ballerini, M., Cabibbo, N., Candelier, R., Cavagna, A., Cisbani, E., Giardina, I., Lecomte, V., Orlandi, A., Parisi, G., Procaccini, A., Viale, M., & Zdravkovic, V. (2008). Interaction ruling animal collective behavior depends on topological rather than metric distance: evidence from a field study. *Proceedings of the National Academy of Sciences of the United States of America*, *105*, 1232–7.
- Blue, V. J., & Adler, J. L. (2001). Cellular automata microsimulation for modeling bi-directional pedestrian walkways. *Transportation Research Part B-Methodological*, *35*, 293–312.
- Boltes, M., & Seyfried, A. (2013). Collecting pedestrian trajectories. *Neurocomputing*, *100*, 127–133.
- Boltes, M., Seyfried, A., Steffen, B., & Schadschneider, A. (2010). Automatic extraction of pedestrian trajectories from video recordings. *Pedestrian and Evacuation Dynamics 2008*, (pp. 43–54).
- Boltes, M., Zhang, J., Tordeux, A., Schadschneider, A., & Seyfried, A. (2019). Empirical results of pedestrian and evacuation dynamics. *Complex Dynamics of Traffic Management*, (pp. 671–699).
- Douthwaite, J. A., Zhao, S., & Mihaylova, L. S. (2019). Velocity obstacle approaches for multi-agent collision avoidance. *Unmanned Systems*, *7*, 55–64.
- Fiorini, P., & Shiller, Z. (1998). Motion planning in dynamic environments using velocity obstacles. *The International Journal of Robotics Research*, *17*, 760–772.
- Fortune, S. (1987). A swepline algorithm for voronoi diagrams. *Algorithmica*, *2*, 153–174.
- Fu, Z., Jia, Q., Chen, J., Ma, J., Han, K., & Luo, L. (2018). A fine discrete field cellular automaton for pedestrian dynamics integrating pedestrian heterogeneity, anisotropy, and time-dependent characteristics. *Transportation Research Part C: Emerging Technologies*, *91*, 37–61.
- Hart, P. E., Nilsson, N. J., & Raphael, B. (1968). A formal basis for the heuristic determination of minimum cost paths. *IEEE transactions on Systems Science Cybernetics*, *4*, 100–107.
- Helbing, D., Buzna, L., Johansson, A., & Werner, T. (2005). Self-organized pedestrian crowd dynamics: Experiments, simulations, and design solutions. *Transportation Science*, *39*, 1–24.
- Helbing, D., Farkas, I., & Vicsek, T. (2000). Simulating dynamical features of escape panic. *Nature*, *407*, 487–90.
- Helbing, D., & Johansson, A. (2009). Pedestrian, crowd and evacuation dynamics. In *Encyclopedia of complexity and systems science* (pp. 6476–6495). Springer.
- Helbing, D., & Molnar, P. (1995). Social force model for pedestrian dynamics. *Physical Review E*, *51*, 4282–4286.
- Khambhaita, H., & Alami, R. (2020). Viewing robot navigation in human environment as a cooperative activity. In N. M. Amato, G. Hager, S. Thomas, & M. Torres-Torriti (Eds.), *Robotics Research* (pp. 285–300). Springer International Publishing.

- Ma, Y., Lee, E. W., Hu, Z., Shi, M., & Yuen, R. K. (2019). An intelligence-based approach for prediction of microscopic pedestrian walking behavior. *IEEE Transactions on Intelligent Transportation Systems*, (pp. 1–17).
- Moussaid, M., Helbing, D., & Theraulaz, G. (2011). How simple rules determine pedestrian behavior and crowd disasters. *Proceedings of the National Academy of Sciences of the United States of America*, *108*, 6884–8.
- Older, S. (1968). *Movement of pedestrians on footways in shopping streets*. Traffic engineering and control.
- Pandey, A., Pandey, S., & Parhi, D. (2017). Mobile robot navigation and obstacle avoidance techniques: A review. *Int Rob Auto J*, *2*, 00022.
- Seyfried, A., Steffen, B., Klingsch, W., & Boltes, M. (2005). The fundamental diagram of pedestrian movement revisited. *Journal of Statistical Mechanics: Theory and Experiment*, *2005*, P10002.
- Van Den Berg, J., Guy, S. J., Lin, M., & Manocha, D. (2011). Reciprocal n-body collision avoidance. In *Robotics research* (pp. 3–19). Springer.
- Weidmann, U. (1993). *Transporttechnik der Fussgänger: Transporttechnische Eigenschaften des Fussgängerverkehrs (Literaturauswertung)*. ETH, IVT.
- Xiao, Y., Chraïbi, M., Qu, Y., Tordeux, A., & Gao, Z. (2018). Investigation of voronoi diagram based direction choices using uni- and bi-directional trajectory data. *Physical Review E*, *97*, 052127.
- Xiao, Y., Gao, Z. Y., Qu, Y. C., & Li, X. G. (2016). A pedestrian flow model considering the impact of local density: Voronoi diagram based heuristics approach. *Transportation Research Part C-Emerging Technologies*, *68*, 566–580.
- Xiao, Y., Xu, J., Chraïbi, M., Zhang, J., & Gou, C. (2022). A generalized trajectories-based evaluation approach for pedestrian evacuation models. *Safety Science*, *147*, 105574.
- Zhang, P., Ouyang, W., Zhang, P., Xue, J., & Zheng, N. (2019). Sr-lstm: State refinement for lstm towards pedestrian trajectory prediction. In *Proceedings of the IEEE Conference on Computer Vision and Pattern Recognition* (pp. 12085–12094).

Appendix A. Detour coefficient

The detour coefficient σ_i is meant to indicate the difficulty level of the future journey to the destination, and here it is indicated according to the potential conflicts using a geometric approach. The approach can be described with two steps as follows.

Step 1: The identification of potential conflicting point. For the object pedestrian P_0 (see Fig. A.1), the neighboring pedestrians are divided into two types depending on that whether the destination is clear or not. For the first type of pedestrian whose destination is clear, the potential conflicting point is identified by judging the intersection between two segments from the pedestrian to the destination (e.g., segment $\overline{P_0D_0}$ and segment $\overline{P_1D_1}$). For the second type whose destination is unclear for the object pedestrian, the potential conflicting point is the intersection between the segment of object pedestrian and the velocity ray of the related pedestrian (e.g., segment $\overline{P_0D_0}$ and ray v_2). Note that in many cases no potential conflicting point is identified when there is no intersection point.

Step 2: The calculation of potential conflict. For each conflicting point, the conflicting time gap is calculated by $\Delta t_{ij} = \left| d_i^j / v_i - d_j^i / v_j \right|$, where d_i^j and d_j^i respectively denotes the distance of pedestrian P_i and P_j to the conflicting point. Accordingly, the detour coefficient σ_i is calculated as,

$$\sigma_i = \sum_j e^{-\Delta t_{ij} / D_i}, \quad (\text{A.1})$$

where D_i indicates the distance between pedestrian P_i to the corresponding destination.

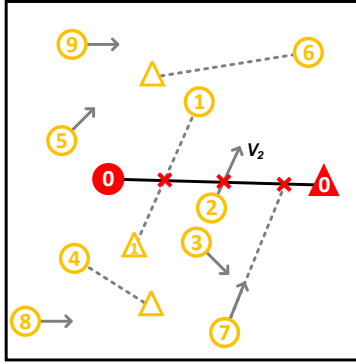


Figure A.1: Sketch map of the estimated detour degree.